

UPCommons

Portal del coneixement obert de la UPC

<http://upcommons.upc.edu/e-prints>

Aquesta és una còpia de la versió *author's final draft* d'un article publicat a la revista Carbohydrate polymers.

URL d'aquest document a UPCommons E-prints:
<http://hdl.handle.net/2117/116423>

Article publicat / *Published paper:*

Facundo Beltramino, M. Blanca Roncero, Teresa Vidal, Cristina Valls.
(2018) A novel enzymatic approach to nanocrystalline cellulose preparation. Carbohydrate Polymers, vol. 189. p. 39-47. Doi: 10.1016/j.carbpol.2018.02.015

1 **A novel enzymatic approach to nanocrystalline cellulose preparation**

2 Beltramino, Facundo; Roncero, M. Blanca; Vidal, Teresa; Valls, Cristina*

3 CELBIOTECH_Paper Engineering Research Group. Universitat Politècnica de

4 Catalunya (UPC. BarcelonaTech). Colom 11, E-08222, Terrassa, Spain

5 Facundo Beltramino: facundo.beltramino@upc.edu

6 M.Blanca Roncero: blanca.roncero@upc.edu

7 Teresa Vidal: teresa.vidal@upc.edu

8

9

10

11

12

13

14 Correspondence to:

15 C. Valls

16 CELBIOTECH_Paper Engineering Research Group. Universitat Politècnica de Catalunya,
17 BarcelonaTech, C/Colom, 11, 08222 Terrassa, Spain.

18 E-mail: crisrina.valls@upc.edu

19 Tel: +34 937398147

20 Fax: +34 937398101

21

22 **Abstract**

23 In this work, conditions for an enzymatic pretreatment prior to NCC isolation from cotton linter
24 were assessed. Different cellulase doses and reaction times were studied within an experimental
25 design and NCC were obtained. At optimal enzymatic conditions (20U, 2h), a total yield greater
26 than 80% was achieved and the necessary enzymatic treatment time was reduced 90%. Different
27 intensities of enzymatic treatments led to proportional decreases in fiber length and viscosity
28 and also were inversely proportional to the amount of released oligosaccharides. These
29 differences within fibers lead to quantitative differences in NCC: increase in acid hydrolysis
30 yield, reduction of NCC surface charge and crystallinity increase. Benefits produced by
31 enzymatic treatments did not have influence over other NCC characteristics such as their sulfur
32 content ($\approx 1\%$), size (≈ 200 nm), zeta potential (≈ -50 mV) or degree of polymerization (≈ 200).
33 Evidence presented in this work would reduce the use of harsh sulfuric acid generating a cleaner
34 stream of profitable oligosaccharides.

35

36

37

38

39

40

41

42

43

44 **Keywords:** Nanocrystalline cellulose; Cellulase; Optimization; Yield increase; fiber length

1. Introduction

Research in nanocrystalline cellulose (NCC), a material also named cellulose nanocrystals, started some years ago (Rånby, 1951; Revol, Bradford, Giasson, Marchessault, & Gray, 1992) and has generated a huge interest in recent years due to the promising features this material holds (Habibi, Lucia, & Rojas, 2010; Sun et al., 2014; Trache, Hussin, Haafiz, & Thakur, 2017). Typically, it consists on a rigid rod-like monocrySTALLINE cellulose domain with dimensions among 1-100 nm in width and up to several hundred nanometers in length (Lin & Dufresne, 2014). Also, they are produced from cellulose fibers, a very abundant raw material (Zhu et al., 2016). NCC has a high degree of crystal structure, a high aspect ratio (length-to-diameter, up to 300), a large surface area (above $150 \text{ m}^2 \text{ g}^{-1}$), a very high elastic moduli, (estimated to be over 130-150 GPa) and a low thermal expansion coefficient (6 ppm K^{-1}) (Tanaka, Saito, Ishii, & Isogai, 2014). This material finds many potential applications in diverse fields such as an additive for composite materials (Moon, Martini, Nairn, Simonsen, & Youngblood, 2011), optical applications (Lin, Huang, & Dufresne, 2012), or diverse uses in biomedicine (Lin & Dufresne, 2014), to name a few.

Biotechnology has been used for several applications in cellulose industry, such as biobleaching, biorefining, or even pulp quality upgrades (Beltramino, Valls, Vidal, & Roncero, 2015; Beltramino, 2016; Garcia-Ubasart, Torres, Vila, Pastor, & Vidal, 2013; Quintana, Valls, Vidal, & Blanca Roncero, 2013; Valls & Roncero, 2009). Generally, the use of enzymes as a green technology allows reducing the pollution generated by traditional chemical processes, providing a solution for an enormous social concern. Cellulases, enzymes degrading cellulose include three different enzymatic activities (Teixeira et al., 2015). Endoglucanases (E.C. 3.2.1.4) catalyze the hydrolysis of the 1, 4-glycosidic linkages of the amorphous regions of cellulose. In nature, they hydrolyze cellulose in synergy with cellobiohydrolases (E.C. 3.2.1.91), which act upon the reducing and non-reducing ends of cellulose chains. Finally, β -glucosidases (E.C. 3.2.1.21), catalyze the hydrolysis of cellobiose into glucose. Generally, this enzymatic cellulose degrading activity is capable of participating into NCC preparation, fact that is

73 reflected in some examples of authors successfully introducing enzymes (cellulases) into
74 nanocellulose preparation process (Anderson et al., 2014; Teixeira et al., 2015; Zhang, Xue,
75 Zhang, & Zhao, 2012). The first proposal of the concept of using enzymes for producing
76 cellulose nanomaterials was stated by Zhu, Sabo, & Luo, 2011. Furthermore, enzymatic
77 preparation of NCC has been related with an improved quality of final product compared to
78 pure chemical processes (George, Ramana, Bawa, & Siddaramaiah, 2011).

79 One of the main drawbacks associated with NCC preparation is the low yield presented by the
80 typical acid hydrolysis with sulfuric acid used for its preparation (Chen et al., 2015).

81 Considering this evidence, a previous work from our group demonstrated that a cellulase
82 pretreatment on cotton linters could increase the yield of NCC as well as to influence other
83 characteristics of them (Beltramino, Roncero, Vidal, Torres, & Valls, 2015). Optimizations via
84 factorial designs have been widely used in literature for optimizing enzymatic and chemical
85 treatments for diverse applications (Bondeson, Mathew, & Oksman, 2006; Fillat & Roncero,
86 2009, 2010; Valls & Roncero, 2009). In a previous study, conditions of sulfuric acid hydrolysis
87 in order to maximize NCC yield from cellulase-pretreated fibers were optimized using a
88 factorial design (Beltramino, Roncero, Torres, Vidal, & Valls, 2016). Maximal yield was
89 achieved with 25 minutes of hydrolysis at 47°C and using 62% wt. H₂SO₄. In the light of the
90 results formerly obtained, this work intended to find the best conditions for obtaining the
91 maximum profit of enzyme action. For this, conditions for the enzymatic pretreatment were
92 optimized before and after obtaining NCC within a 2² complete factorial design. The main
93 objective was to maximize the yield of the whole enzymatic and chemical process. We focused
94 into the assessment of quantitative effects of these pretreatments of different intensity and their
95 relations in both cellulose fibers and NCC. The purpose of this study was to find the best
96 conditions for the enzymatic pretreatment providing the highest NCC yield in combination with
97 optimal conditions established in a previously reported work (Beltramino, Roncero, Torres,
98 Vidal, & Valls, 2016).

99 2. Materials and methods

100

101 2.1. Cellulose source and enzyme

102 Cotton linters provided by Celsur (Spain) were used as a raw material for experiments.
103 Composition of fibers was: glucans content (cellulose) $97.7\% \pm 0.3$; xylans content $2\% \pm 0.2$;
104 Rhamnans $0.2\% \pm 0.15$; acetyl groups $0.1\% \pm 0.1$. Fibers, as received from provider, were
105 beaten in a valley mill for 90 minutes for reducing average length. Obtained fibers were named
106 as “initial”. A **commercial** cellulase preparation (named “C”), provided by Fungal Bioproducts
107 (Spain) and obtained from *Cerreña sp.* fungus was used for treatments. **Previous works**
108 **demonstrate that it is not a mono-component enzyme (Beltramino, Valls, Vidal, & Roncero,**
109 **2015; Beltramino, 2016).** Activity as $U\ g^{-1}$ from enzyme stock was 1700 and was expressed as
110 CMCase units *i.e.* the amount of enzyme degrading $1\ \mu\text{mol}$ of CMC (carboxymethylcellulose)
111 per minute.

112 2.2. Enzymatic treatments

113

114 Enzymatic treatments were held using cellulase C on an Ahiba Easydye (Datacolor, USA)
115 apparatus having independent 250 mL vessels with agitation consisting on upside-down
116 inversions at 20 oscillations per minute. Treatments were performed at 55°C , 5% consistency
117 and pH 5 maintained with a 50 mM sodium acetate buffer solution **on distilled water**. Enzyme
118 dose and reaction time were variables chosen in accordance to an experimental design (Table 1).
119 After reactions a liquor sample was recovered for residual enzymatic activity determination and
120 enzyme was deactivated by heating samples to 105°C during 15 min. Fibers were then filtered
121 using a filter with pore size $N^{\circ}2$ and reaction liquor was passed through fibers 3 times in order
122 to recover fines. No washing was performed after treatments in order to avoid sample loss and
123 samples of reaction liquor were saved for sugar content analysis. A control for enzymatic
124 treatments was also performed on fibers, applying the same conditions as for treatments during
125 2h, but with no enzyme addition.

126 **2.2.1. Experimental design**

127

128 Enzymatic treatments were applied in accordance to a 2² statistical factorial plan involving two
129 levels and two variables plus three repetitions in the central point, which required a total of 7
130 experiences (Table 1). Variables were: X1(enzyme dose), varied within 2 – 20 U g⁻¹ odp (oven-
131 dried pulp) range and X2 (reaction time) varied within 2 – 24 h. These independent variables
132 were coded as -1 or +1; both for direct comparison of coefficients and to better understand the
133 effect of each variable on the responses. The results of the three repetitions at the central point
134 and their variance were used in combination with the variance of the saturated model to
135 calculate Snedecor’s F-value in order to determine whether the variance was homogeneous or
136 heterogeneous. Since the variance was homogeneous in all cases, a linear model was
137 constructed, its significant terms identified and potential curvature detected. Two additional
138 points were required for solving quadratic terms confounding. Linear multiple regression
139 technique was applied by using an Microsoft Excel spreadsheet to implement the stepwise
140 backward regression method and discard all terms with a probability (p-value) less than 0.05.

141 **Table 1.** Experiences of the statistical plan with their conditions

Y	X1	X2	Cellulase dose (U g ⁻¹ odp)	Enzymatic treatment time (h)
Y1	-1	-1	2	2
Y2	1	-1	20	2
Y3	-1	1	2	24
Y4	1	1	20	24
Y5	0	0	11	13
Y6	0	0	11	13
Y7	0	0	11	13
Y8	1	0	20	13
Y9	0	-1	11	2

142

143 **2.3. Nanocrystalline cellulose preparation**

144

145 Nanocrystalline cellulose (NCC) was obtained from initial, control and enzymatically pretreated
146 fibers by a controlled sulfuric acid hydrolysis, using the protocol proposed by Dong et al., 1998.
147 Fibers were fluffed prior to hydrolysis, oven dried and cooled in a desiccator. Typically, 1.5 g of

148 sample weighted immediately from desiccator was hydrolyzed with 62 % (w/w) sulfuric acid
149 for 25 min at 47 °C with an acid-to-fibers ratio of 10:1 (*i.e.* 10 mL g⁻¹ cellulose), optimal
150 hydrolysis conditions described in a previous work (Beltramino, Roncero, Torres, Vidal, &
151 Valls, 2016). In all cases, hydrolysis reaction was stopped by diluting the acid with chilled (4°C)
152 distilled water in a 10-fold basis, and also cooling samples immediately on an ice bath. Samples
153 were then centrifuged at 6000 rpm for 15m and supernatant was discarded. Samples were re
154 suspended in distilled water and centrifugation step was repeated, discarding supernatant.
155 Samples were then sonicated to disperse them using a Hielscher UP100H ultrasonic processor at
156 100% amplitude and 0.75 cycles for 20 min on an ice bath to prevent heating which may cause
157 desulfation (Dong et al., 1998). Re suspended samples were then dialyzed against distilled water
158 using a 10kDa Thermo Fischer dialysis membrane until pH 3. Final samples were filtered
159 through Whatman ashless paper filters, N° 41 (pore size 20-25 µm).

160 **2.4. Samples characterization**

161 **2.4.1. Cellulose fibers**

162 Enzymatic treatment yield was calculated by determining the solid residue (treated fibers) after
163 treatments and was indicated as % of recovered fibers mass. Initial and enzymatically treated
164 fibers were characterized in terms of viscosity and fiber length according to ISO 5351:2010, and
165 TAPPI Standard T271, respectively.

166 Infrared spectra of fibers samples were recorded at room temperature using a Perkin Elmer
167 Spectrum 100 ATR-FTIR spectrophotometer. Fourier transformed infrared spectroscopy (FTIR)
168 spectral analysis was conducted within the wavenumber range of 600-4000 cm⁻¹. A total of 64
169 scans were run to collect each spectrum at a 1cm⁻¹ resolution. Total crystallinity index (TCI) as
170 proposed by Nelson and O`Connor (Nelson & O`Connor, 1964) was estimated from the ratio
171 between the absorption peaks at 1370 cm⁻¹ and 2900 cm⁻¹, respectively.

172 **2.4.2. Enzymatic treatment effluents**

173 Released reducing sugars on enzymatic reaction effluents were analyzed using a 1100 Agilent
174 HPLC instrument (Agilent technologies, USA) furnished with a BIO RAD Aminex HPX-42A
175 ion-exchange column. Residual enzymatic activity on effluents was determined using an
176 adapted version of Somogyi-Nelson method to determine reducing sugar concentrations on a
177 solution (Spiro, 1966).

178 **2.4.3. Nanocrystalline cellulose**

179 Yield NCC isolation by acid hydrolysis was determined drying 25 mL of the suspension and
180 determining the mass after evaporation at 60°C in an air circulating oven. Solids content was
181 calculated and yield was expressed as % of initial fiber mass. Values were given as average of
182 three independent determinations for each sample.

183 Sulfur content of NCC was determined according to a procedure proposed by Abitbol et al.
184 (Abitbol, Kloser, & Gray, 2013). Briefly, a small sample of suspension was titrated using 1.25
185 mM NaOH recording conductivity values. The equivalence point corresponded to the amount of
186 NaOH necessary to neutralize all the sulfate groups attached to crystals surface. Results were
187 calculated as % of mass of atomic sulfur over NCC mass. Values are given as average of three
188 independent measurements for each sample.

189 Particle size of NCC samples (**Z average**) as well as **polydispersity index (PDI)** were determined
190 using a DL135 particle size analyzer (Cordouan Technologies, France). Size distribution was
191 determined with dynamic light scattering (DLS) at room **temperature** (25°C). Aqueous
192 suspensions were placed directly in the measuring cell and laser power was adjusted for
193 counting around 2000 particles per minute.

194 Surface charge of suspensions of fibers and NCC was determined using Müttek particle charge
195 detector (PCD03PH, Müttek, Germany). Suspensions were titrated using 0,001N Poly-Dadmac
196 (cationic poly-electrolyte). Surface charge density was calculated according to the following
197 formula (Cadena, García, Vidal, & Torres, 2009) :

198
$$\text{Surface charge } \left(\frac{\text{meq}}{\text{g}} \right) = \frac{VxC}{wt}$$

199 Where V and C are the volume and the concentration of the titration agent (poly-dadmac),
200 respectively, and wt is the weight of the NCC sample.
201 Zeta potential (electrophoretic mobility) of aqueous NCC suspensions was determined using
202 Malvern Zetamaster (ZEM, Malvern instruments, UK) from which data was averaged over 6
203 measurements. All samples were analyzed at room temperature.
204 NCC degree of polymerization (DP) was determined using a modified version of ISO
205 5351:2010, using 0.2-0.3 g of dried NCC suspensions as samples. The degree of polymerization
206 was calculated from the intrinsic viscosity $[\eta]$, using the equation of (SCAN-CM 15:88):
207 $DP^{0.085}=1.1 [\eta]$.
208 FTIR spectra of dried NCC films were recorded following the same procedure as for fibers. TCI
209 was also calculated from spectra.

210 **3. Results and discussion**

211 The effects produced by the enzyme were analyzed and optimized before and after obtaining the
212 NCC in order to evaluate if quantitative differences in enzymatic effects on fibers led to
213 proportional differences in NCC. This kind of optimization had not been performed before.

214 **3.1. Modelling enzymatic treatment response on fibers**

215 Due to the degrading nature of cellulase action, a loss of cellulose mass is associated to these
216 enzymatic treatments, fact that must be taken into account when considering process yield. In
217 the same direction, cellulase action strongly reduced average fiber length. For studying this,
218 values of enzymatic treatment yield and fiber length were found to fit Equation 1 and 2,
219 respectively. As shown by equations, both responses were affected by both individual variables
220 and also by the quadratic term of reaction time, being it the most influential one. Data predicted
221 by models showed that enzymatic yield and fiber length suffered a great variation from 2 hours
222 to ≈ 11 hours, in which a yield loss of ≈ 10 points (Figure 1A) and a ≈ 1 mm reduction of fiber
223 length (Figure 1B) were produced. On the other hand, enzyme dose had a smaller influence than
224 reaction time in both parameters, particularly in enzymatic treatment yield. At 2 h of treatment,

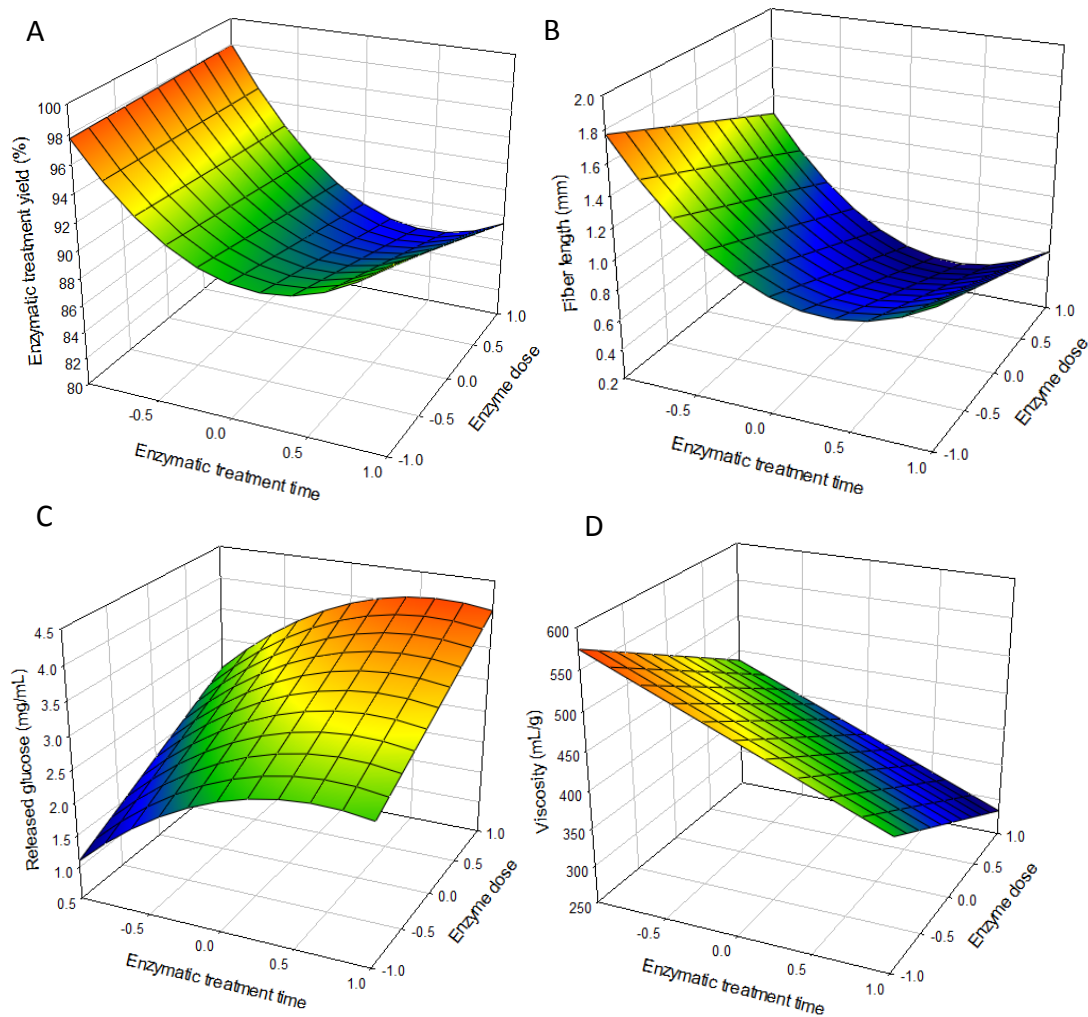
225 the reduction in fiber length produced by increasing enzyme dose did not produce a noticeable
226 loss in fiber mass.

227 Enzymatic treatment yield (%) = $88.4 - 1.4 X_1 - 3.8 X_2 - 1.6 X_1X_2 + 5.7 X_2^2$ $R^2 = 0.93$

228 **Equation 1**

229 Fiber length (mm) = $0.71 - 0.25 X_1 - 0.33 X_2 + 0.48 X_2^2$ $R^2 = 0.95$

230 **Equation 2**



231

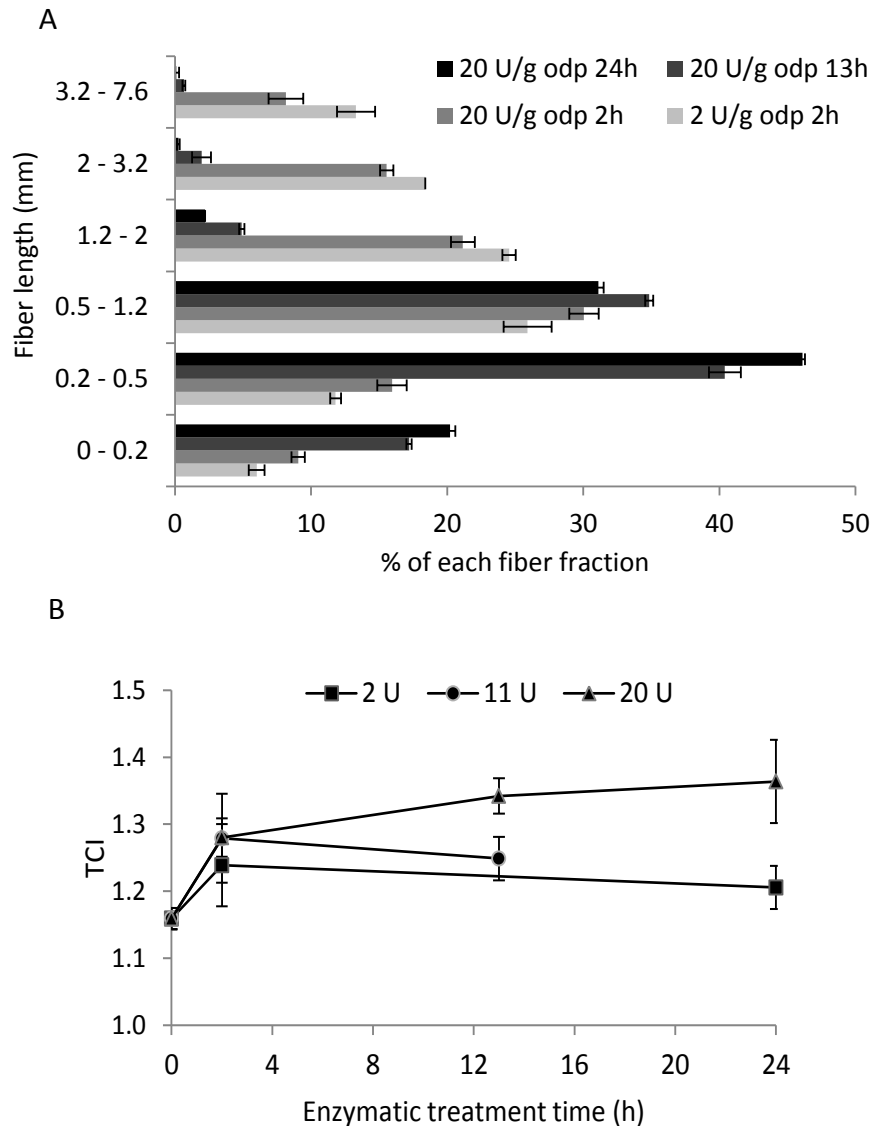
232 **Figure 1:** Models relating enzymatic treatment yield (A), fiber length (B), total released glucose
233 (C) and fiber viscosity (D) to enzyme dose and enzymatic treatment time.

234

235 In order to fully understand the effects of enzymatic treatments in fiber length, the distribution

236 among different measures was studied and illustrated in Figure 2A. Comparing samples at 2 h

237 of treatment, increase in enzyme from 2 to 20 U g⁻¹ odp dose slightly reduced the amount of
238 fibers above 1.2 mm while it increased the amount of the ones below this length. In turn,
239 reaction time produced a major effect, as previously observed, strongly reducing the presence of
240 fibers longer than 1.2 mm and thereafter increasing the presence of shorter ones. The action
241 pattern of enzyme in the reduction of fiber length seemed to be the same for increases in
242 enzyme dose or reaction time. However, the magnitude of the effects of the increase in the
243 former was much smaller than the one of the latter. This fact could explain that no loss in
244 cellulose mass was associated to increases in enzyme dose although a small reduction in length
245 was observed.



246

247 **Figure 2:** Fiber length distribution of samples after enzymatic treatments (A). Total crystallinity
 248 index (TCI) of fibers during enzymatic treatments (B)

249

250 Oligosaccharides released as a consequence of enzymatic treatments were expressed as glucose
 251 equivalents after the molar addition of each oligosaccharide multiplied by their number of
 252 glucose units. These values fitted Equation 3. For this response a similar effect to that of yield
 253 and fiber length was observed (Figure 1C). A large increase in glucose concentration was
 254 observed from 2 hours to ≈ 11 hours of treatment, up to $\approx 4 \text{ mg mL}^{-1}$, observing stabilization after
 255 this period. In this case, enzyme dose had a linear effect, smaller than that of reaction time and
 256 independent of it, increasing sugar concentration all along enzymatic treatment. On the other
 257 hand, fibers viscosity values fitted Equation 4. In it, the quadratic term of reaction time was not

258 found to affect the response and a linear surface was obtained (Figure 1D). Viscosity decreased
259 as enzymatic treatment intensity increased with a minimum value obtained at the point of the
260 most intensive enzymatic conditions, *i.e.* 20 U g⁻¹ odp and 24 hours, accounting for a 50%
261 reduction of viscosity.

$$262 \quad \text{Released glucose (mg mL}^{-1}\text{)} = 3.17 + 0.71 X_1 + 0.77 X_2 - 0.59 X_2^2 \quad R^2 = 0.93$$

263 **Equation 3**

$$264 \quad \text{Viscosity (mL g}^{-1}\text{)} = 429 - 69 X_1 - 76 X_2 \quad R^2 = 0.93$$

265 **Equation 4**

266 Enzymatic treatments also increased cellulose crystallinity, expressed as total crystallinity index
267 (TCI). Data indicated that fibers TCI (Figure 2B) increased as a consequence of higher enzyme
268 doses, while reaction time did not seem to produce any effect **after 2h**. Generally, this
269 crystallinity increase indicates that a higher amount of crystalline cellulose was present on fibers
270 after enzymatic treatments. The explanation of this might be found in the reduction in
271 amorphous cellulose regions caused by cellulase preferential attack on them. This preference is
272 due to the larger accessibility presented by β -1,4 glycosidic bonds in these domains (Tȃta et al.,
273 2015).

274 **3.2. Enhancing enzymatic effects on nanocrystalline cellulose**

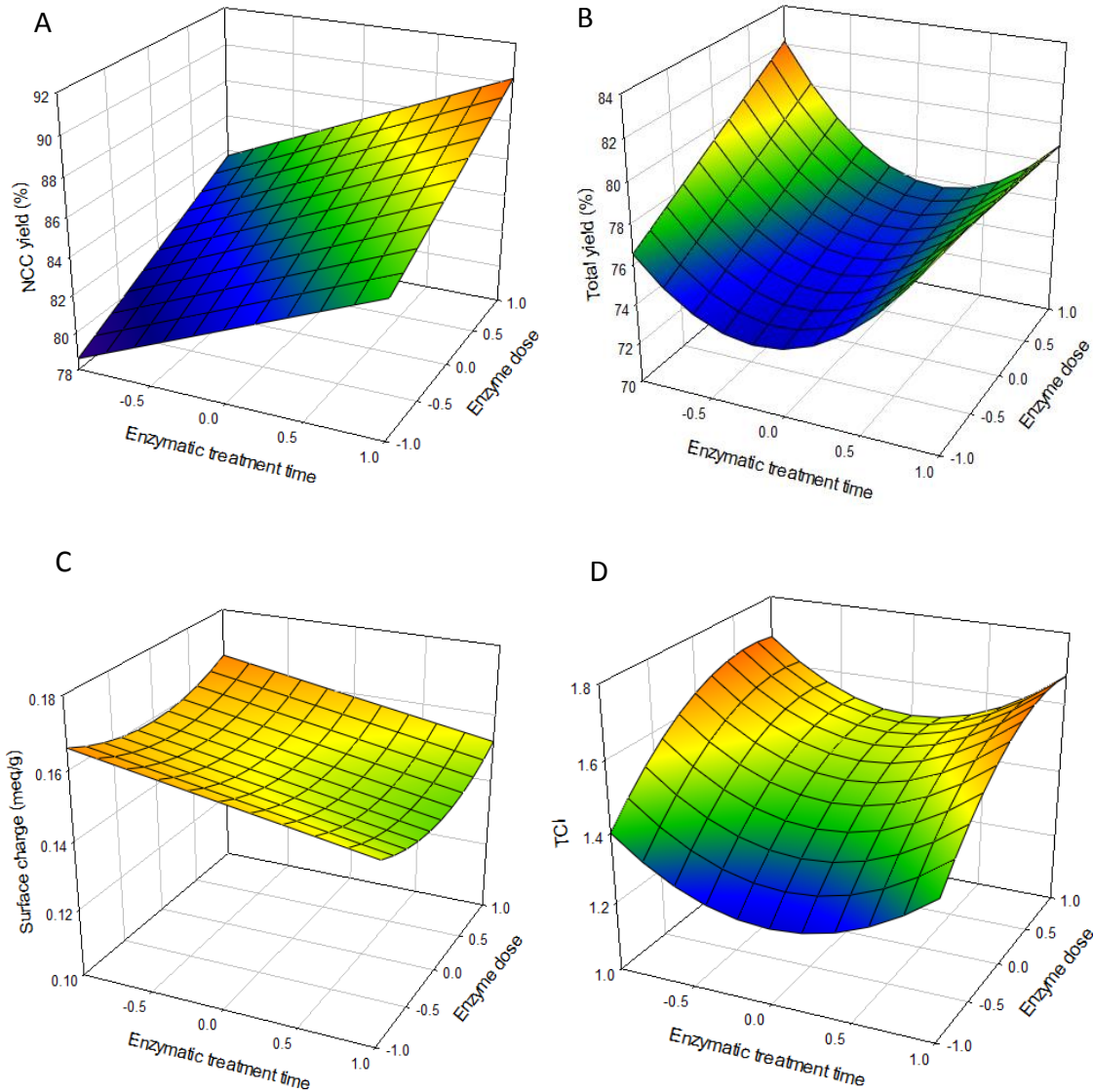
275 **3.2.1. Modelling enzymatic treatment response on nanocrystalline cellulose**

276 Low yields traditionally attributed to NCC isolation raised interest in the study of ways for its
277 increase, in order to increment the industrial feasibility of this process (Chen et al., 2015; Fan &
278 Li, 2012). NCC yield values from sulfuric acid hydrolysis fitted the model indicated in Equation
279 5, showing that it was positively influenced by both independent variables studied in this work.
280 Cellulase pretreatment increased the yield of sulfuric acid hydrolysis up to a 90%, with a larger
281 effect produced by reaction time (Figure 3A). NCC yield model revealed a linear inverse
282 correlation to the model presented by fibers viscosity. The minimal and maximal values of NCC
283 yield were shown by 2 U g⁻¹ odp, 2 h and 20 U g⁻¹ odp, 24 h samples, respectively. These

284 samples also showed the maximal and minimal fiber viscosity and fiber length values,
285 respectively. This suggested that a higher depolymerization and shortening of fibers by cellulase
286 was the cause for the increase in the yield of NCC hydrolysis.

287
$$\text{NCC yield (\%)} = 84.4 + 2.6 X_1 + 3.3 X_2 \quad R^2 = 0.97.$$

288 **Equation 5**



289 **Figure 3:** Model relating: NCC hydrolysis yield (A), Total yield (B), NCC surface charge (C)
290 and NCC total crystallinity index (TCI) (D) to enzyme dose and enzymatic treatment time.
291
292

293 As stated in introduction and considering evidence previously exposed, calculation of total
294 yield, as combined enzymatic and acid hydrolysis yields becomes crucial for acknowledging a

295 real value of the outcome of the NCC isolation process. A compromise solution between the
296 gain in the NCC yield and the loss of fibers mass both due to enzymatic pretreatment must be
297 found. Total yield values were found to fit Equation 6. **In this equation, compared to the model**
298 **expressed in Equation 5, individual influence of enzyme dose decreased. On the other hand,**
299 **treatment time influenced only in the quadratic term and double-interacting with the enzyme**
300 **dose.** Total yield (Figure 3B) had a minimum value at around 11 h of treatment, coinciding with
301 the point of stabilization of enzyme effect on fibers, showing higher values with shorter and
302 longer times. This was explained by yields of both enzymatic and sulfuric acid hydrolysis
303 (Figure 1A and Figure 3A). At short reaction times the loss in cellulose mass by enzymatic
304 treatments was small, while with extended treatments, cellulose mass loss was compensated by
305 higher gains in NCC hydrolysis yield.

$$\text{Total yield (\%)} = 74.6 + 1.2 X_1 - 1.6 X_1 X_2 + 4.7 X_2^2 \quad R^2 = 0.98$$

Equation 6

308 Surface charge of NCC was found to fit Equation 7. As can be observed, it was negatively
309 influenced by enzymatic reaction time and positively by the quadratic term of enzyme dose. It
310 was observed that surface charge of NCC was slightly reduced with longer enzymatic
311 pretreatments (Figure 3C), while enzyme dose produced no significant affectation. This charge
312 reduction was in accordance with previous observations (Beltramino, Roncero, Torres, Vidal,
313 & Valls, 2016; Beltramino, Roncero, Vidal, Torres, & Valls, 2015) where enzymatic effects
314 seemed to reduce this parameter.

$$\text{Surface charge (meq g}^{-1}\text{)} = 0.152 - 0.007 X_2 + 0.007 X_1^2 \quad R^2 = 0.79$$

Equation 7

317 Crystallinity values of NCC, as TCI fitted Equation 8. TCI of NCC was affected by enzyme
318 dose linearly and by quadratic terms of both variables. In Figure 3D it can be observed how
319 enzymatic pretreatment on fibers led to NCC with a higher crystallinity. Data shows that TCI
320 was majorly increased by enzyme dose with values tending to stabilize after a $\approx 10 \text{ U g}^{-1} \text{ odp}$
321 dose. However, no significant effect was found to be produced by enzymatic reaction time, a

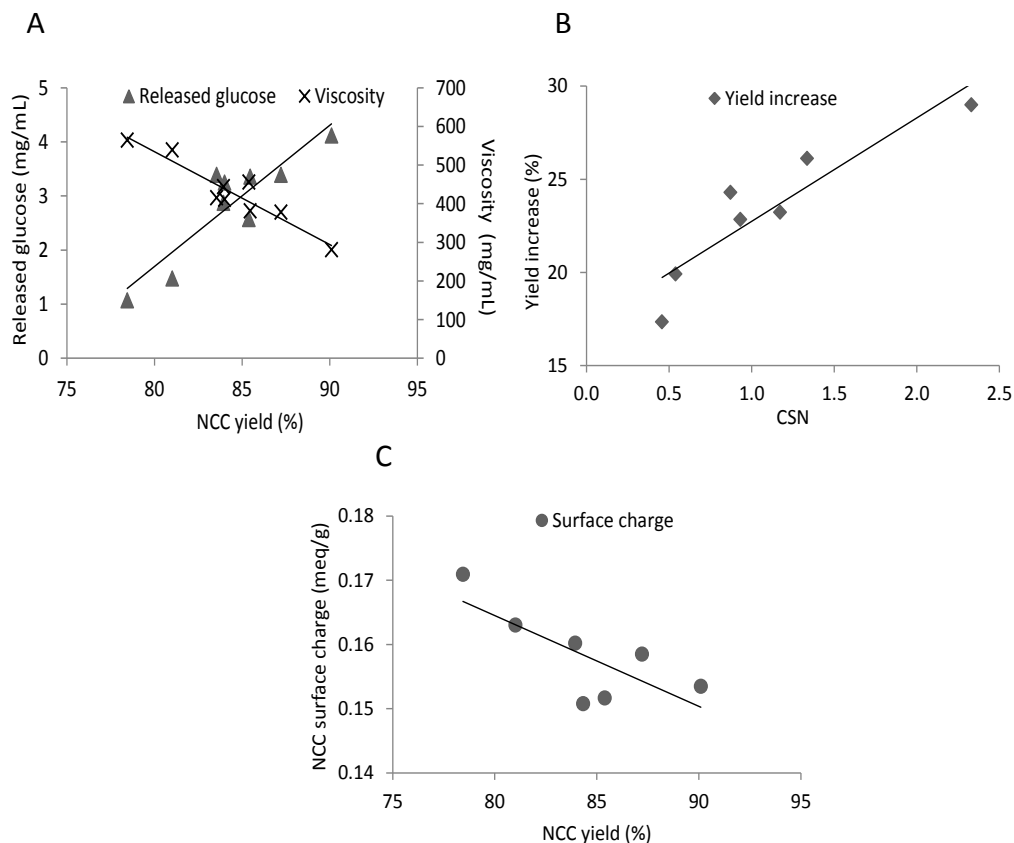
322 similar behavior to that observed in TCI of fibers. Also, it is important to remark that the
323 optimal point of the process concerning total yield ($20 \text{ U g}^{-1} \text{ odp}$, 2h) corresponded to NCC with
324 the higher crystallinity, providing further evidence of the quality increase produced by this
325 enzymatic-aided process.

326
$$\text{TCI} = 1.46 + 0.14 X_1 - 0.1 X_1^2 + 0.18 X_2^2 \quad R^2 = 0.99$$

327 **Equation 8**

328 The observation of former data also foregrounded the fact that quantitative differences in
329 enzymatic treatment intensity led to quantitative differences in NCC features. This statement is
330 well illustrated in Figure 4A, where it can be observed how NCC hydrolysis yield is linearly
331 correlated to fibers viscosity (inverse correlation) and also to total released glucose (as glucose
332 equivalents). Also, with the aim of further illustrating this, Figure 4B correlates chain scission
333 number (CSN), *i.e.* the average number of cuts produced in cellulose chains with the increase in
334 yield derived from enzymatic action. The correlation between both parameters indicated again
335 that a higher number of cuts, *i.e.* a stronger enzymatic action, corresponded to a greater increase
336 in yield. Finally, the reduction of NCC electrical charge produced by the enzyme is well
337 illustrated in Figure 4C, where larger NCC yields (*i.e.* larger enzymatic effects) led to smaller
338 values of surface charge, agreeing with data exposed in Figure 3C.

339



340

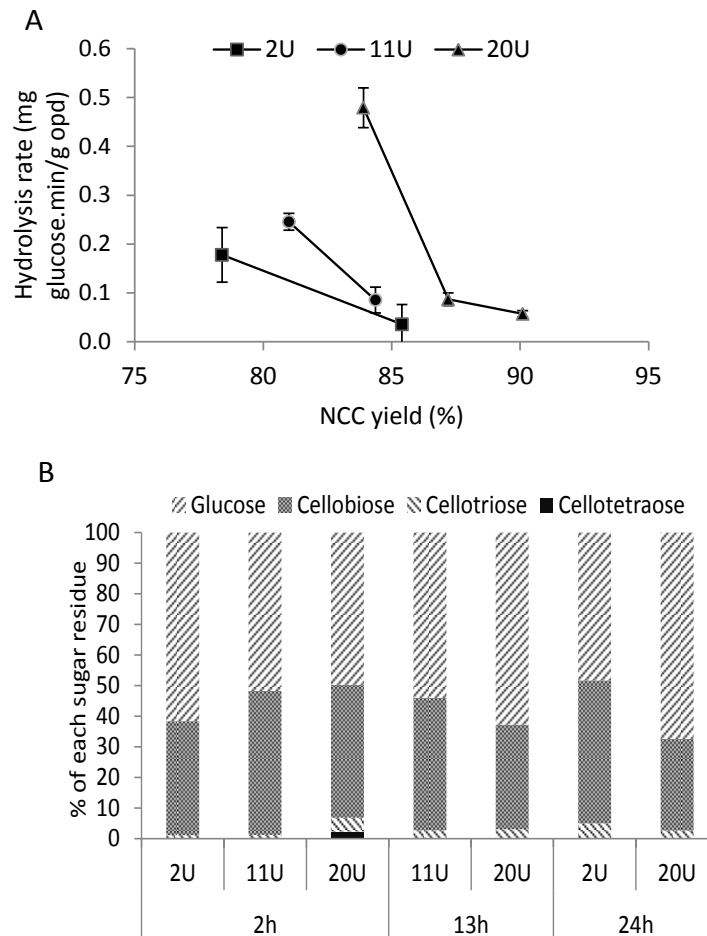
341 **Figure 4:** Cellulase quantitative effects. Total released sugars (as glucose equivalents) and
 342 fibers viscosity expressed in front of NCC yield (A), NCC yield increase expressed versus chain
 343 scission number (CSN), both calculated from initial fibers (B) and NCC surface charge
 344 expressed versus NCC yield (C).

345 3.2.2. Studying enzymatic reaction effluents

346

347 Enzymatic hydrolysis rate, calculated dividing the total glucose equivalents produced during
 348 each enzymatic treatment by the total duration of the treatment (in minutes), is illustrated in
 349 Figure 5A in front of the hydrolysis yield obtained from each sample. For all enzymatic doses,
 350 highest hydrolysis rates were found at 2 h, with higher values at a higher dose. From this point,
 351 extending treatment up to 24 h time seemed to reduce hydrolysis rate. This reduction was
 352 possibly due to the increase in oligosaccharides concentration on reaction media, compounds
 353 which are known to be capable of act as cellulase inhibitors (Nguyen, Neo, & Yang, 2015).
 354 Interestingly, the maximal hydrolysis rate, *i.e.*, the point of maximal hydrolytic efficiency, was
 355 found at 2 h of treatment and with 20 U g⁻¹ odp. This point was also found to be the optimal for
 356 cellulase application as it offered the highest total yield, showing a correlation between

357 efficiency of the entire process and of enzymatic catalysis. Furthermore, in order to validate
 358 these results, residual activity (as % of initial dose) was measured. After 24 hours of treatment,
 359 2 U g⁻¹ odp and 20 U g⁻¹ odp samples showed activity conservation values of 55% ± 10 and 24%
 360 ± 4, confirming that the enzyme was still active after 24 h and thereafter validating data shown
 361 in Figure 5A.



362

363 **Figure 5:** Enzymatic hydrolysis rate, as mg glucose released per minute as a consequence of
 364 enzymatic treatments expressed in front NCC hydrolysis yield (A). Proportion of each
 365 oligosaccharide released during enzymatic hydrolysis (B).
 366

367

368 Concerning the different sugar species found in effluents (Figure 5B), in the first place, a small
 369 amount of xylose was found. This presence was product of a xylanolytic activity present on
 370 cellulase preparation and proceeded of the hydrolysis of the small amount of xylans initially

371 present on fibers. In the second place, concerning glucose-oligosaccharides, glucose was found
372 to be the main released sugar, followed by cellobiose and cellotriose, in a decreasing amount.
373 Differences in enzyme dose led to a variation of glucose-oligosaccharides. Generally, higher
374 enzymatic doses led to the release of longer oligosaccharides within two hours of treatment, fact
375 well illustrated by the finding of cellotetraose only in one sample. Meanwhile, reaction time
376 seemed to tend to reestablish the original proportions among oligosaccharides, *i.e.* $\approx 67\%$
377 glucose, $\approx 30\%$ cellobiose and $\approx 3\%$ cellotriose.

378 **3.2.3. NCC sulfur content, size and stability**

379

380 NCC surface charge is responsibility of charged sulfate moieties introduced on their surface
381 during sulfuric acid hydrolysis (Abitbol et al., 2013; Peyre et al., 2015). Sulfur content data of
382 NCC (Table 2) failed to show quantitative reductions produced by cellulase pretreatment, as
383 observed for surface charge. Nevertheless, it could be observed that compared to initial fibers,
384 enzymatic pretreatment on fibers led to NCC with lower sulfur content. In addition, sulfate
385 groups on NCC are known to increase the thermodegradability of the material (Roman &
386 Winter, 2004) making the reduction produced by cellulase a positive modification for NCC
387 quality.

388 Another NCC parameter, suspension stability, is critical in the preparation of nanocomposites
389 (Filson, Dawson-Andoh, & Schwegler-Berry, 2009). This stability is indicated by the absolute
390 value of zeta potential (electrophoretic mobility) of suspensions and is promoted by the negative
391 charge of sulfate groups on crystals surface (Peyre et al., 2015). Table 2 shows zeta potential
392 values, being all them among -50 mV indicating high suspension stability, which seemed to be
393 maintained regardless of the enzymatic treatment performed. A similar behavior was shown by
394 PDI, as all suspensions showed a narrow particle size distribution.

395 Concerning NCC dimensions, it was observed that different intensities of enzymatic
396 pretreatment did not produce any modification in average particle size of resulting NCC (Table
397 2). With this, it was highlighted that the benefits of cellulase pretreatment did not result in

398 deleterious modifications in the morphology of NCC. Also, this fact was already observed (
 399 Beltramino, Roncero, Torres, Vidal, & Valls, 2016) when cellulase pretreatment produced no
 400 affectation on NCC size with 62% wt. sulfuric acid. However, in a different study, a slight size
 401 increase in NCC was produced by enzymatic pretreatment (Beltramino, Roncero, Vidal, Torres,
 402 & Valls, 2015). This evidence remarks again the fact that the effects of enzymatic pretreatment
 403 are largely dependent on the acid hydrolysis conditions, which were modified within these
 404 studies.

405 Finally, the degree of polymerization (DP) of cellulose chains in NCC was calculated from
 406 viscosity values (Table 2). DP of NCC did not seem to be modified by enzymatic treatments,
 407 observing in all cases that cellulose chains were formed by ≈ 200 glucose units. These values
 408 were similar to those reported by other authors for NCC obtained via sulfuric acid hydrolysis
 409 (Satyamurthy, Jain, Balasubramanya, & Vigneshwaran, 2011).

410 **Table 2:** NCC sulfur content, electrophoretic mobility, polydispersity index (PDI), average size
 411 and degree of polymerization (DP).

		Sulfur content (% S)	Zeta Potential (mV)	PDI	Z average (nm)	DP
Initial		1.21 ± 0.03	-47.2 ± 0.6	0.18 ± 0.04	205 ± 4	183 ± 17
Control 2h		1.12 ± 0.06	-49.1 ± 0.7	0.19 ± 0.03	184 ± 19	200 ± 25
2 U	2 h	1.22 ± 0.02	-46.7 ± 0.7	0.19 ± 0.01	191 ± 25	188 ± 6
	24 h	1.12 ± 0.04	-48.2 ± 0.4	0.18 ± 0.03	206 ± 7	193 ± 17
11 U	2 h	0.99 ± 0.01	-49.3 ± 0.7	0.18 ± 0.04	199 ± 4	193 ± 12
	13 h	1.03 ± 0.04	-49.4 ± 0.5	0.19 ± 0.01	206 ± 5	179 ± 12
	13 h	0.92 ± 0.01	-48.7 ± 0.4	0.17 ± 0.02	204 ± 13	173 ± 21
	13 h	0.87 ± 0.01	-48.5 ± 0.6	0.19 ± 0.02	209 ± 24	210 ± 12
20 U	2 h	0.99 ± 0.05	-48.9 ± 0.7	0.20 ± 0.01	206 ± 10	208 ± 26
	13 h	1.03 ± 0.03	-48.9 ± 0.6	0.19 ± 0.02	195 ± 9	203 ± 14
	24 h	1.05 ± 0.01	-48.2 ± 0.7	0.19 ± 0.02	183 ± 14	198 ± 41

412
 413
 414

3.3. Optimal point and models verification

415 As stated in previous sections, the objective of this work was to find the optimal conditions for
 416 enzymatically pretreating fibers in order to produce the largest possible total NCC yield. Thus,
 417 the optimal point of the cellulase combined with acid hydrolysis was found at: 20 U g⁻¹ odp

418 cellulase dose and 2 h of treatment, producing a $\approx 82\%$ total yield, 21 points higher than that of
419 NCC obtained from initial fibers. This total yield was similar to that reported by Tang et al.,
420 (2013) using a non-conventional preparation procedure obtaining NCC esterified with acetic
421 acid. Also, it was noticeably bigger than other optimal values reported using sulfuric acid
422 hydrolysis (Chen et al., 2015; Fan & Li, 2012). **Moreover, compared to a previous study**
423 **(Beltramino, Roncero, Torres, Vidal, & Valls, 2016) this optimization allowed reducing in a**
424 **90% the required enzymatic treatment time, although the enzyme dose was duplicated.** In
425 addition, if increasing enzyme dose resulted unaffordable, a total yield of $\approx 79\%$ was obtained
426 using a $\approx 11 \text{ U g}^{-1}$ odp dose and 2 hours of treatment, representing a loss of 3 points in total yield
427 but a smaller enzyme dose. This strong reduction would increase the industrial feasibility of this
428 greener process, as industry is usually reluctant to long treatments. Accordingly, enzyme
429 showed the largest hydrolysis rate *i.e.* the one using more efficiently its potential, at 20 U g^{-1}
430 odp and at 2 hours of treatment, conditions defined as optimal. In other words, this optimization
431 meant a reduction of the hydrolysis of biomass mediated by sulfuric acid in benefit of an
432 efficient enzymatic catalysis. Furthermore, sugars present on effluents as a result of NCC
433 manufacture could be used as a feedstock, for example, for bioethanol conversion (Brinchi,
434 Cotana, Fortunati, & Kenny, 2013). In this case, enzymatic hydrolysis effluents permit an easier
435 usage than those produced by sulfuric acid hydrolysis, due to the absence of sulfuric acid in
436 them, highlighting another benefit of the proposed enzymatic-assisted process.

437 Finally, with the aim of verifying the obtained models, new samples were prepared using the
438 optimal cellulase conditions plus another sample with a 20 U g^{-1} odp dose and 24 h of treatment,
439 which led to a total yield of $\approx 79\%$ and thereafter was also interesting. Table 3 shows data
440 obtained from these new samples and also the predicted data by models. As can be observed,
441 new values were in all cases in accordance with those predicted by models or similar to previous
442 experimental data.

443

444 **Table 3:** Characterization of samples for models verification. New experimental values and
 445 those predicted by models are indicated. *When no model was found fitting data, previous
 446 experimental data is indicated.

Fibers	20U 2h		20U 24h	
	Predicted*	Observed	Predicted*	Observed
Enzymatic treatment yield (%)	98	96.3	87.4	85.8
Fiber length (mm)	1.27	1.28 ± 0.04	0.61	0.48 ± 0.02
Viscosity (mL g ⁻¹)	436.1	457 ± 28	283.7	296 ± 12
Released glucose (mg mL ⁻¹)	2.52	2.62 ± 0.09	4.06	4.3 ± 0.19
TCI*	1.28 ± 0.03	1.25 ± 0.02	1.36 ± 0.06	1.30 ± 0.06
NCC				
NCC yield (%)	83.7	84.5 ± 0.8	90.2	89.8 ± 0.8
Total yield (%)	82.2	81.4	78.9	77.1
Surface charge (meq g ⁻¹)	0.166	0.172 ± 0.005	0.152	0.156 ± 0.004
TCI	1.68	1.61 ± 0.1	1.68	1.65 ± 0.16
Sulfur content (% S)*	0.99 ± 0.05	1.1 ± 0.09	1.05 ± 0.01	0.94 ± 0.05
Z average (nm)*	206 ± 10	186 ± 11	183 ± 14	204 ± 8
Z potential (mV)*	-48.9 ± 0.7	-49.6 ± 0.5	-48.2 ± 0.7	-50.7 ± 0.8
PDI*	0.2 ± 0.1	0.21 ± 0.02	0.19 ± 0.02	0.2 ± 0.02
DP*	208 ± 26	198 ± 18	198 ± 41	203 50

447

448 4. Conclusions

449

450 Evidence presented in this work allowed finding the optimal enzymatic conditions for NCC
 451 isolation in combination with optimal sulfuric acid hydrolysis ones from a previous work (25
 452 minutes of hydrolysis at 47°C and 62% wt. H₂SO₄). Now, an enzyme dose of 20 U g⁻¹ odp and
 453 2h of hydrolysis allowed reaching a total NCC yield of ≈82%. This outcome was found to be 12
 454 **percentage** points higher to that of NCC from control fibers and 21 **percentage** points higher
 455 than that of NCC obtained from initial ones. Also, this optimization reduced the necessary
 456 enzymatic treatment time in a 90% (from 24h to 2h) compared to former studies, boosting the
 457 industrial feasibility of this greener technology. Furthermore, enzymatic pretreatment showed to
 458 increase NCC crystallinity and to slightly reduce their surface charge, not affecting other
 459 characteristics. We found that quantitative differences in enzymatic effects on fibers led to
 460 proportional differences in NCC. The use of optimal enzymatic conditions would permit to
 461 reduce the use of harsh corrosive sulfuric acid for NCC production while generating a more
 462 easily exploitable stream of oligosaccharide-rich effluents.

463 **Acknowledgements**

464 Authors are grateful to "Ministerio de Economía y Competitividad" (Spain) for their support in
465 this work under the FILMBIOCEL CTQ2016-77936-R (funding also from the "Fondo Europeo
466 de Desarrollo Regional FEDER"), BIOPAP μ FLUID CTQ2013-48995-C2-1-R,
467 MICROBIOCEL CTQ2017-84966-C2-1-R projects and a FPI grant (BES-2011-046674) to
468 Facundo Beltramino. Special thanks are also due to the consolidated research group AGAUR
469 2014 SGR 534 with Universitat de Barcelona (UB) and to the Serra Húnter Fellow to Cristina
470 Valls. We are also grateful to Celsur and Fungal Bioproducts for supplying cotton linters and
471 enzyme, respectively.

472

473 **5. References**

- 474 Abitbol, T., Kloser, E., & Gray, D. G. (2013). Estimation of the surface sulfur content of
475 cellulose nanocrystals prepared by sulfuric acid hydrolysis. *Cellulose*, 20(2), 785–794.
476 <http://doi.org/10.1007/s10570-013-9871-0>
- 477 Anderson, S. R., Esposito, D., Gillette, W., Zhu, J. Y., Baxa, U., & McNeil, S. E. (2014).
478 Enzymatic preparation of nanocrystalline and microcrystalline cellulose. *Tappi Journal*,
479 13(5), 35–42.
- 480 **Beltramino, F. (2016). Enzymatic-assisted preparation of nanocrystalline cellulose from non-**
481 **wood fibers. *PhD thesis*. Universitat Politècnica de Catalunya.**
482 **<http://hdl.handle.net/10803/404447>**
- 483 Beltramino, F., Roncero, M. B., Torres, A. L., Vidal, T., & Valls, C. (2016). Optimization of
484 sulfuric acid hydrolysis conditions for preparation of nanocrystalline cellulose from
485 enzymatically pretreated fibers. *Cellulose*, 23, 1777–1789. [http://doi.org/10.1007/s10570-](http://doi.org/10.1007/s10570-016-0897-y)
486 [016-0897-y](http://doi.org/10.1007/s10570-016-0897-y)
- 487 Beltramino, F., Roncero, M. B., Vidal, T., Torres, A. L., & Valls, C. (2015). Increasing yield of
488 nanocrystalline cellulose preparation process by a cellulase pretreatment. *Bioresource*
489 *Technology*, 192, 574–581. <http://doi.org/10.1016/j.biortech.2015.06.007>
- 490 Beltramino, F., Valls, C., Vidal, T., & Roncero, M. B. (2015). Exploring the effects of
491 treatments with carbohydrases to obtain a high-cellulose content pulp from a non-wood
492 alkaline pulp. *Carbohydrate Polymers*, 133, 302–312.
493 <http://doi.org/10.1016/j.carbpol.2015.07.016>
- 494 Bondeson, D., Mathew, A., & Oksman, K. (2006). Optimization of the isolation of nanocrystals
495 from microcrystalline cellulose by acid hydrolysis. *Cellulose*, 13(2), 171–180.
496 <http://doi.org/10.1007/s10570-006-9061-4>

497 Brinchi, L., Cotana, F., Fortunati, E., & Kenny, J. M. (2013). Production of nanocrystalline
498 cellulose from lignocellulosic biomass: technology and applications. *Carbohydrate*
499 *Polymers*, 94(1), 154–69. <http://doi.org/10.1016/j.carbpol.2013.01.033>

500 Cadena, E. M., García, J., Vidal, T., & Torres, A. L. (2009). Determination of zeta potential and
501 cationic demand in ECF and TCF bleached pulp from eucalyptus and flax. Influence of
502 measuring conditions. *Cellulose*, 16, 491-500.

503 Chen, L., Wang, Q., Hirth, K., Baez, C., Agarwal, U. P., & Zhu, J. Y. (2015). Tailoring the
504 yield and characteristics of wood cellulose nanocrystals (CNC) using concentrated acid
505 hydrolysis. *Cellulose*, 22(3), 1753–1762. <http://doi.org/10.1007/s10570-015-0615-1>

506 Dong, X. M., Revol, J.-F., & Gray, D. G. (1998). Effect of microcrystallite preparation
507 conditions on the formation of colloid crystals of cellulose. *Cellulose*, 5(1), 19–32.

508 Fan, J., & Li, Y. (2012). Maximizing the yield of nanocrystalline cellulose from cotton pulp
509 fiber. *Carbohydrate Polymers*, 88(4), 1184–1188.
510 <http://doi.org/10.1016/j.carbpol.2012.01.081>

511 Filson, P. B., Dawson-Andoh, B. E., & Schwegler-Berry, D. (2009). Enzymatic-mediated
512 production of cellulose nanocrystals from recycled pulp. *Green Chemistry*, 11, 1808–1814.
513 <http://doi.org/10.1039/b915746h>

514 Fillat, U., & Roncero, M. B. (2009). Biobleaching of high quality pulps with laccase mediator
515 system: Influence of treatment time and oxygen supply. *Biochemical Engineering Journal*,
516 44, 193-198. <http://doi.org/DOI: 10.1016/j.bej.2008.12.002>

517 Fillat, U., & Roncero, M. B. (2010). Optimization of laccase–mediator system in producing
518 biobleached flax pulp. *Bioresource Technology*, 101(1), 181–187. [http://doi.org/DOI:
519 10.1016/j.biortech.2009.07.020](http://doi.org/DOI: 10.1016/j.biortech.2009.07.020)

520 Garcia-Ubasart, J., Torres, A. L., Vila, C., Pastor, F. I. J., & Vidal, T. (2013). Biomodification
521 of cellulose flax fibers by a new cellulase. *Industrial Crops and Products*, 44, 71–76.

- 522 George, J., Ramana, K. V., Bawa, a. S., & Siddaramaiah. (2011). Bacterial cellulose
523 nanocrystals exhibiting high thermal stability and their polymer nanocomposites.
524 *International Journal of Biological Macromolecules*, 48(1), 50–57.
525 <http://doi.org/10.1016/j.ijbiomac.2010.09.013>
- 526 Habibi, Y., Lucia, L. a, & Rojas, O. J. (2010). Cellulose nanocrystals: chemistry, self-assembly,
527 and applications. *Chemical Reviews*, 110(6), 3479–500. <http://doi.org/10.1021/cr900339w>
- 528 Lin, N., & Dufresne, A. (2014). Nanocellulose in biomedicine: Current status and future
529 prospect. *European Polymer Journal*, 59, 302–325.
530 <http://doi.org/10.1016/j.eurpolymj.2014.07.025>
- 531 Lin, N., Huang, J., & Dufresne, A. (2012). Preparation, properties and applications of
532 polysaccharide nanocrystals in advanced functional nanomaterials: a review. *Nanoscale*,
533 4(11), 3274–3294. <http://doi.org/10.1039/c2nr30260h>
- 534 Moon, R. J., Martini, A., Nairn, J., Simonsen, J., & Youngblood, J. (2011). Cellulose
535 nanomaterials review: structure, properties and nanocomposites. *Chemical Society*
536 *Reviews*, 40(7), 3941–94. <http://doi.org/10.1039/c0cs00108b>
- 537 Nelson, M. L., & O'Connor, R. T. (1964). Relation of certain infrared bands to cellulose
538 crystallinity and crystal lattice type. Part II. A new infrared ratio for estimation of
539 crystallinity in celluloses I and II. *Journal of Applied Polymer Science*, 8(3), 1325–1341.
540 <http://doi.org/10.1002/app.1964.070080323>
- 541 Nguyen, L. T., Neo, K. R. S., & Yang, K.-L. (2015). Continuous hydrolysis of carboxymethyl
542 cellulose with cellulase aggregates trapped inside membranes. *Enzyme and Microbial*
543 *Technology*, 78, 34–39. <http://doi.org/10.1016/j.enzmictec.2015.06.005>
- 544 Peyre, J., Pääkkönen, T., Reza, M., & Kontturi, E. (2015). Simultaneous preparation of cellulose
545 nanocrystals and micron-sized porous colloidal particles of cellulose by TEMPO-mediated
546 oxidation. *Green Chemistry*, 17(2), 808–811. <http://doi.org/10.1039/C4GC02001D>

547 Quintana, E., Valls, C., Vidal, T., & Blanca Roncero, M. (2013). An enzyme-catalysed
548 bleaching treatment to meet dissolving pulp characteristics for cellulose derivatives
549 applications. *Bioresource Technology*, *148*, 1–8.
550 <http://doi.org/10.1016/j.biortech.2013.08.104>

551 Rånby, B. G. (1951). III. Fibrous Macromolecular Systems. Cellulose and Muscle. The
552 Colloidal Properties of Cellulose Micelles. *Discussions of the Faraday Society*, *11*, 158–
553 164.

554 Revol, J. F., Bradford, H., Giasson, J., Marchessault, R. H., Gray, D. G. (1992). Helicoidal Self-
555 Ordering of Cellulose Microfibrils in Aqueous Suspension. *International Journal of*
556 *Biological Macromolecules*, *14*(3), 170–172.

557 Roman, M., & Winter, W. T. (2004). Effect of sulfate groups from sulfuric acid hydrolysis on
558 the thermal degradation behavior of bacterial cellulose. *Biomacromolecules*, *5*(5), 1671–
559 1677. <http://doi.org/10.1021/bm034519+>

560 Satyamurthy, P., Jain, P., Balasubramanya, R. H., & Vigneshwaran, N. (2011). Preparation and
561 characterization of cellulose nanowhiskers from cotton fibres by controlled microbial
562 hydrolysis. *Carbohydrate Polymers*, *83*(1), 122–129.
563 <http://doi.org/10.1016/j.carbpol.2010.07.029>

564 Spiro, R. G. R. (1966). Analysis of sugars found in glycoproteins. *Methods in Enzymology*,
565 *566*(C), 3–26. [http://doi.org/10.1016/0076-6879\(66\)08005-4](http://doi.org/10.1016/0076-6879(66)08005-4)

566 Sun, Q., Mandalika, A., Elder, T., Nair, S. S., Meng, X., Huang, F., & Ragauskas, A. J. (2014).
567 Nanocomposite film prepared by depositing xylan on cellulose nanowhiskers matrix.
568 *Green Chemistry*, *16*(7), 3458–3462. <http://doi.org/10.1039/c4gc00793j>

569 Tanaka, R., Saito, T., Ishii, D., & Isogai, A. (2014). Determination of nanocellulose fibril length
570 by shear viscosity measurement. *Cellulose*, *21*, 1581–1589. [http://doi.org/10.1007/s10570-](http://doi.org/10.1007/s10570-014-0196-4)
571 [014-0196-4](http://doi.org/10.1007/s10570-014-0196-4)

572 Tang, L., Huang, B., Lu, Q., Wang, S., Ou, W., Lin, W., & Chen, X. (2013). Ultrasonication-
573 assisted manufacture of cellulose nanocrystals esterified with acetic acid. *Bioresource*
574 *Technology*, 127, 100–105. <http://doi.org/10.1016/j.biortech.2012.09.133>

575 Tąta, A., Sokołowska, K., Świder, J., Konieczna-Molenda, A., Proniewicz, E., & Witek, E.
576 (2015). Study of cellulolytic enzyme immobilization on copolymers of N-vinylformamide.
577 *Spectrochimica Acta Part A: Molecular and Biomolecular Spectroscopy*, 149, 494–504.
578 <http://doi.org/10.1016/j.saa.2015.04.112>

579 Teixeira, R. S. S., Silva, A. S. Da, Jang, J.-H., Kim, H.-W., Ishikawa, K., Endo, T., ... Bon, E.
580 P. S. (2015). Combining biomass wet disk milling and endoglucanase/ β -glucosidase
581 hydrolysis for the production of cellulose nanocrystals. *Carbohydrate Polymers*, 128, 75–
582 81. <http://doi.org/10.1016/j.carbpol.2015.03.087>

583 Trache, D., Hussin, M. H., Haafiz, M. K. M., & Thakur, V. K. (2017). Recent progress in
584 cellulose nanocrystals: sources and production. *Nanoscale*, 9(5), 1763–1786.
585 <http://doi.org/10.1039/C6NR09494E>

586 Valls, C., & Roncero, M. B. (2009). Using both xylanase and laccase enzymes for pulp
587 bleaching. *Bioresource Technology*, 100(6), 2032–2039.
588 <http://doi.org/10.1016/j.biortech.2008.10.009>

589 Zhang, Y., Xue, G. X., Zhang, X. M., & Zhao, Y. (2012). Enzymatic preparation of
590 nanocrystalline cellulose from bamboo fibers. *Advanced Materials Research*, 441, 754–
591 758. <http://doi.org/10.4028/www.scientific.net/AMR.441.754>

592 Zhu, J. Y., Sabo, R., & Luo, X. (2011). Integrated production of nano-fibrillated cellulose and
593 cellulosic biofuel (ethanol) by enzymatic fractionation of wood fibers. *Green Chemistry*,
594 13(5), 1339-1344. <http://doi.org/10.1039/c1gc15103g>

595 Zhu, H., Luo, W., Ciesielski, P. N., Fang, Z., Zhu, J. Y., Henriksson, G., Hu, L. (2016). Wood-
596 Derived Materials for Green Electronics, Biological Devices, and Energy Applications.

597 *Chemical Reviews*, 116(16), 9305–9374. <http://doi.org/10.1021/acs.chemrev.6b00225>

598